**A**

B

Supplemental Figure I. Quantification of Calreticulin in the endothelial cell (EC) and myoendothelial junction (MEJ) via immuno-transmission electron microscopy. A, Representative electron micrograph image of transverse section of thoracodorsal artery showing lumen (L), endothelium (E), smooth muscle (S) and MEJ (outlined with black box) projecting through the internal elastic lamina (IEL). The magnified region indicates gold bead staining for calreticulin at the MEJ (black arrows). Scale bar=0.5μm **B**, Quantification of gold beads per μm^2 in the EC monolayer and MEJ. (n=3 arterioles from 3 C57Bl/6 mice, average of 6.33 pictures per arteriole). Comparison was made using unpaired student's t-test.

IEL + nuclei + calreticulin

Calreticulin Ab #2

Calreticulin Ab conjugated w/Alexa 647 (pseudocolored red)
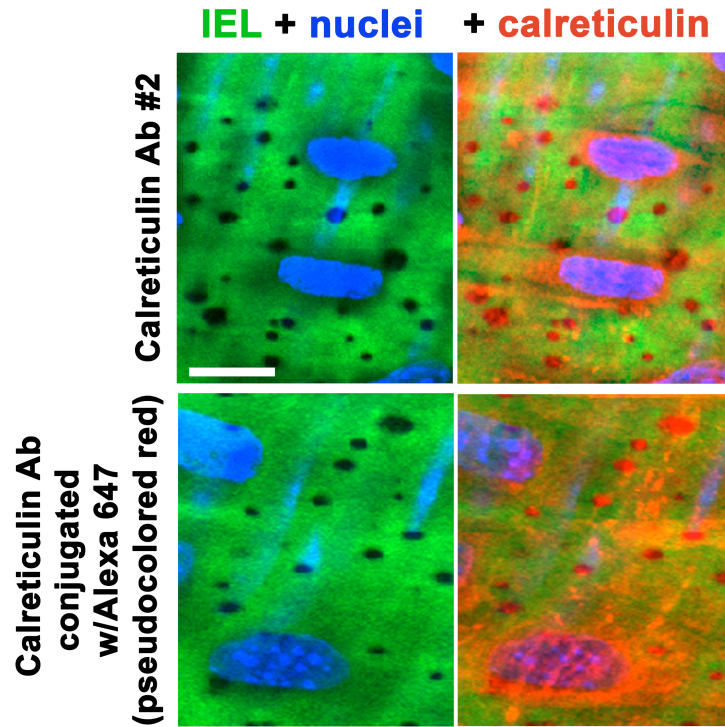
Supplemental Figure II. Validation of immunofluorescence with additional Calr antibodies. Small mesenteric arteries were incubated with antibodies that recognize a different epitope of the Calr protein (versus Thermo Fisher Calr antibody). In images, red is calreticulin, green is IEL, and blue are nuclei. Scale bar= 10mm.

Supplemental Figure III. Z-stack animation of Calr immunofluorescence in EC Calr fl/fl arteriole. Representative spinning disk confocal images of third order mesenteric arteriole. Video starts on the lumenal, EC side and moves in the Z plane in 0.05μm slices towards the abluminal EC, through the IEL and into the SMC and adventitia. Red signal (568 laser) indicates Calr staining and green (488 laser) is autofluorescence from the IEL.

Supplemental Figure IV. Z-stack animation of calreticulin immunofluorescence in EC Calr Δ/Δ arteriole. Representative spinning disk confocal images of third order mesenteric arteriole. Video starts on the lumenal, EC side and moves in the Z plane in 0.05μm slices towards the abluminal EC, through the IEL and into the SMC and adventitia. Red signal (568 laser) indicates Calr staining and green (488 laser) is autofluorescence from the IEL.
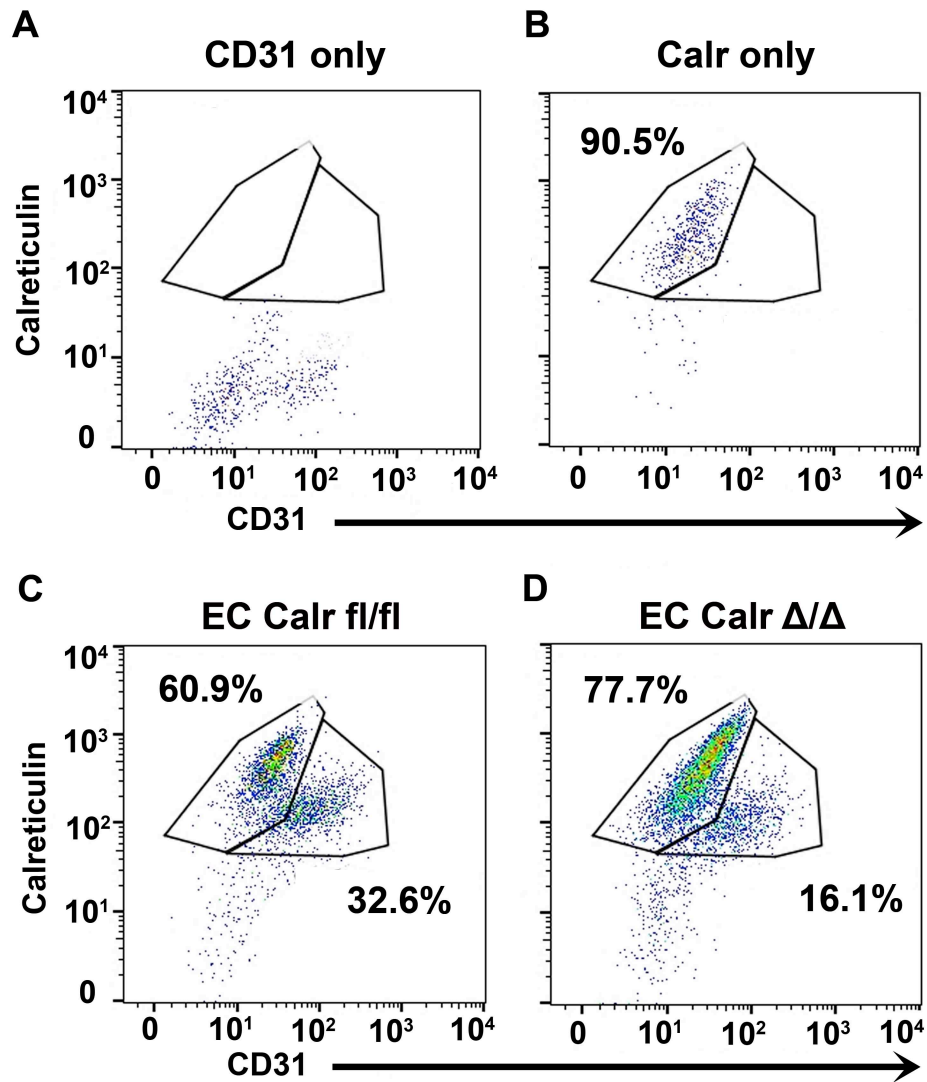
Supplemental Figure V. Representative flow cytometry plots for EC Calr fl/fl and EC Calr Δ/Δ diaphragm. Diaphragms containing microvascular EC were incubated with fluorescent antibodies for **A,** CD31 and **B,** Calreticulin. Then, diaphragm EC from **C,** EC Calr fl/fl and **D,** EC Calr Δ/Δ mice were analyzed for CD31 with expression of Calr.
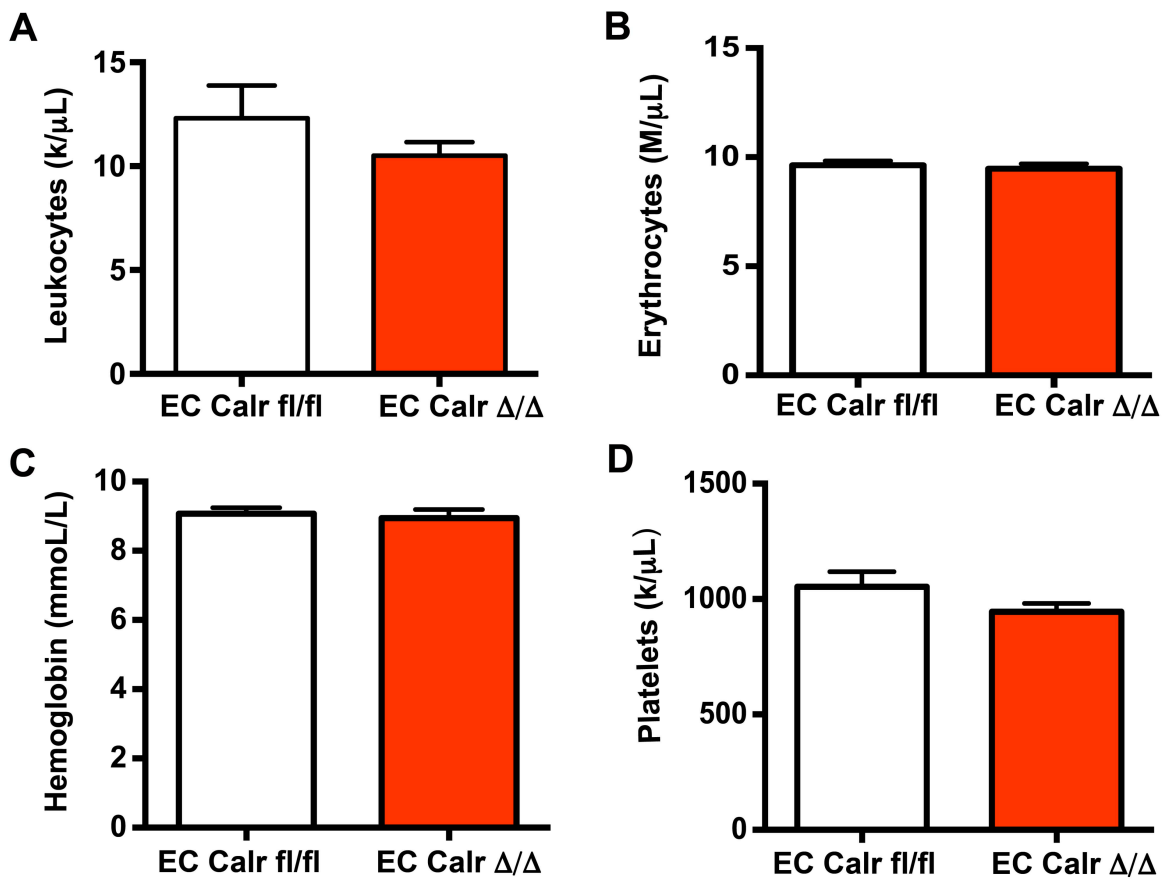
Supplemental Figure VI. EC Calr Δ/Δ does not change blood cell indices. Blood from the retro-orbital sinus was collected from lightly anesthetized EC Calr fl/fl and EC Calr Δ/Δ via microhematocrit tubes and analyzed. Total **A**, leukocytes **B,** erythrocytes **C,** hemoglobin and **D**, platelets are not different between EC Calr fl/fl (n=5) and EC Calr Δ/Δ mice (n=5). Comparison was made uing unpaired student's t-test.
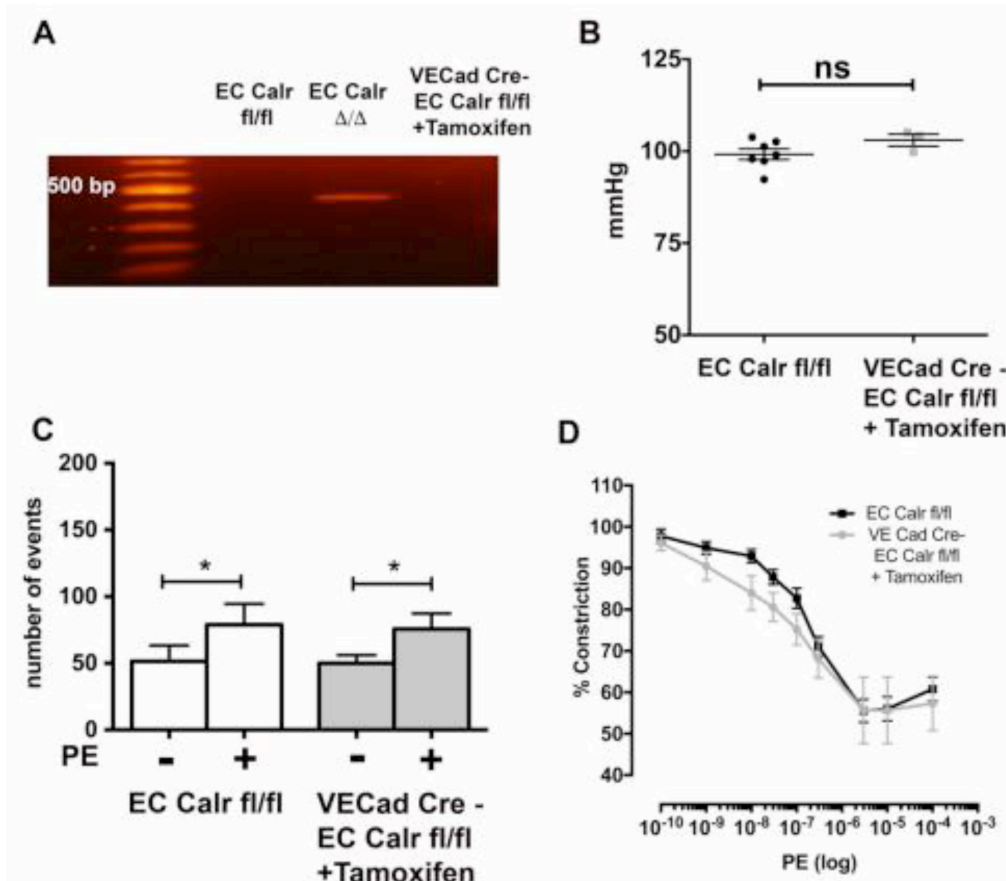
Supplemental VII. Injection of tamoxifen does not affect Calr knockout or cardiovascular function. **A**, Endpoint PCR indicating mice injected with tamoxifen (and without the presence of EC specific cre recombinase) do not have recombination of the Calr gene. **B**, Mean arterial pressure is not different with injection of Tamoxifen. **C**, Calcium events in response to PE are not different. **D**, Vasoreactivity to PE is not significantly different. (Tamoxifen control n=3 for all experiments). Comparisons were made with unpaired student's t-test and C was made with paired student t-test for PE -/+.

Control CCh, 10 μM

Control PE, 10 μM
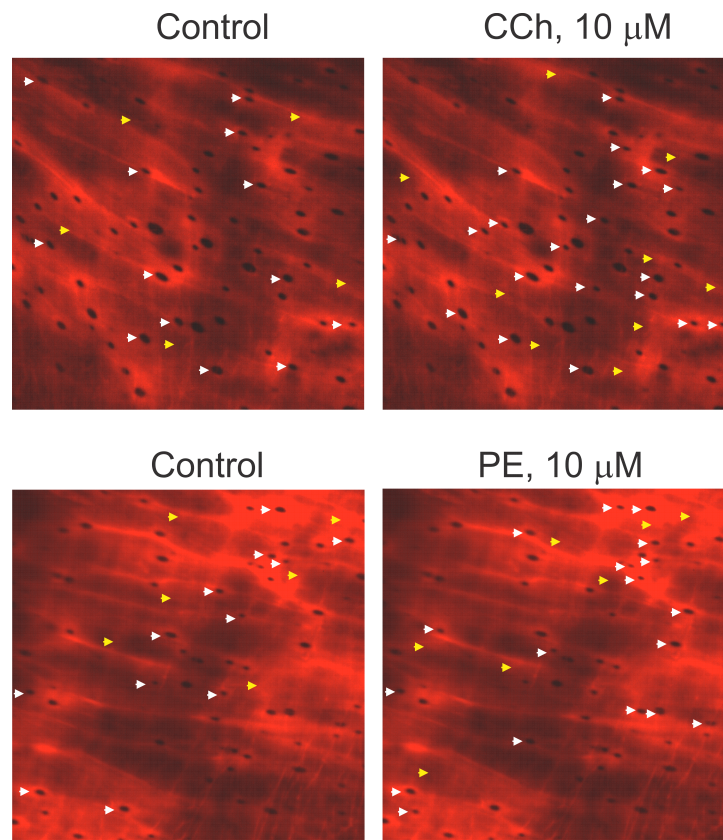
Supplemental Figure VIII. Localization of calcium events. En face mesenteric arteries stained with Alexa Fluor 633 Hydrazide to show holes in the IEL. Regions of interest corresponding to peak fluorescent signals from calcium release events are overlapped with the immunofluorescent images. White arrows indicate location of calcium events that occurred at the IEL holes. Yellow arrows indicate location of calcium events that were outside IEL holes.
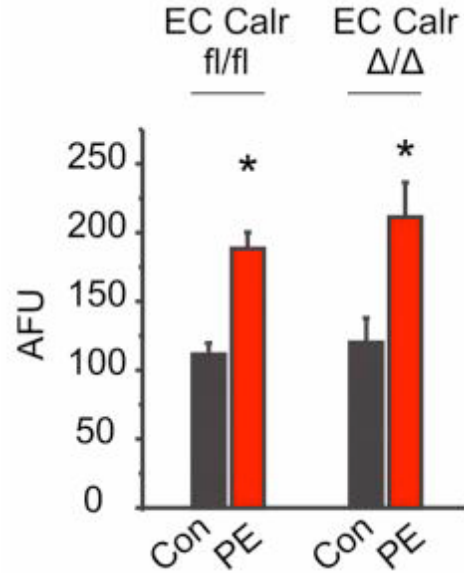
Supplemental Figure IX. EC Calr Δ/Δ does not affect the SMC calcium response to PE.
The SMC response to PE was investigated in mesenteric arteries and presented as arbitrary fluorescent units (AFU). Equivalent increases in calcium fluorescence via Fluo-4 was noted in both groups. * indicates $p < 0.05$ compared to control. Comparisons were made using paired student t-tests.
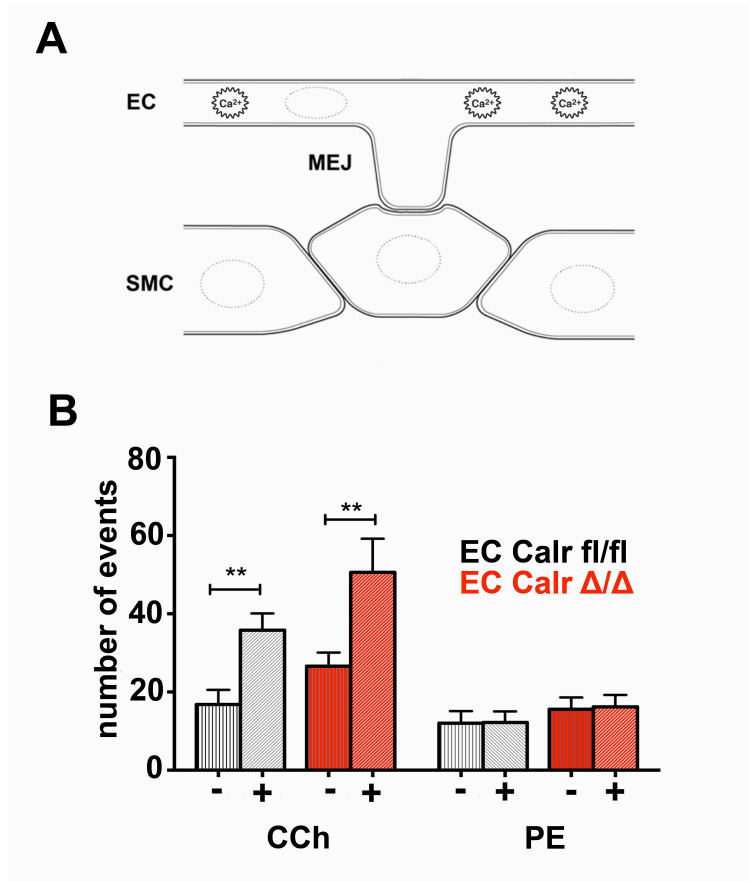
Supplemental Figure X. EC Calr Δ/Δ does not change endothelial monolayer calcium events in response to carbachol. A, Schematic illustrating the calcium events in the EC monolayer that occur outside the MEJ, which are not mediated by phenylephrine (PE). **B,** Carbachol significantly increases calcium events in both groups, while PE has no effect on EC monolayer calcium release (EC Calr fl/fl n=5 arteries from 5 mice; EC Calr Δ/Δ n=5 arteries from 5 mice). ** indicates p<0.01, comparisons were made with paired student's t-tests.
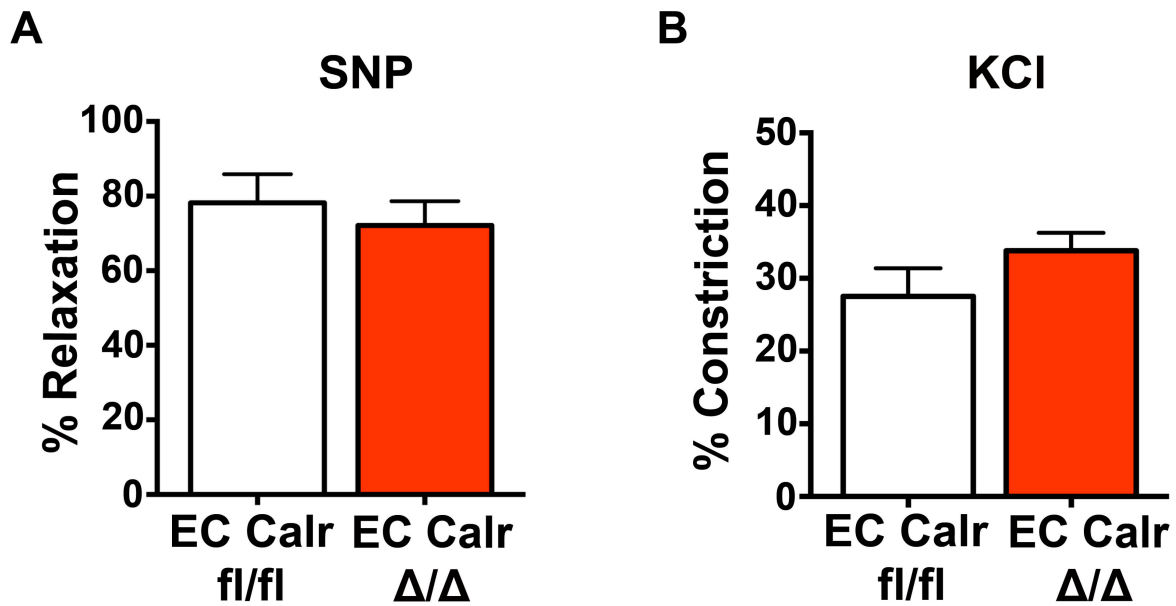
Supplemental Figure XI. EC Calr Δ/Δ does not change endothelial-independent dilation or smooth muscle constriction to KCl. A, Endothelial independent dilation was assessed via 1mM sodium nitroprusside (SNP; EC Calr fl/fl n=9 arteries from 7 mice; EC Calr Δ/Δ n=6 arteries from 5 mice) **B,** SMC constriction was assessed using 40mM KCl (EC Calr fl/fl n=6 arteries from 5 mice; EC Calr Δ/Δ n=8 arteries from 8 mice). Comparisons were made with unpaired student's t-tests.
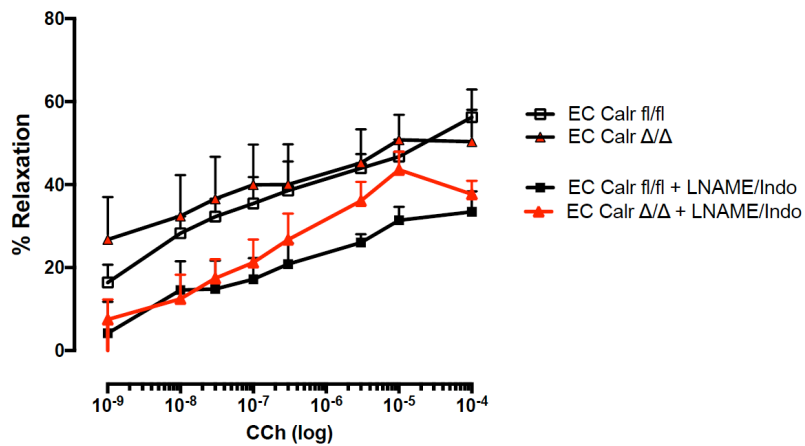
Supplemental Figure XII. EC Calr Δ/Δ mesenteric arteries CCh with L-NAME and indomethacin. Mesenteric arteries were cannulated and pressurized to 80mmHg. Arteries were incubated with L-NAME (to inhibit nitric oxide production) and indomethacin (to inhibit cyclooxygenase and production of prostaglandins) before adding successive doses of CCh. (EC Calr fl/fl +LNAME/Indo n=2 vessels from 2 mice; EC Calr Δ/Δ + L-NAME/Indo n=6 vessels from 5 mice).

A

B
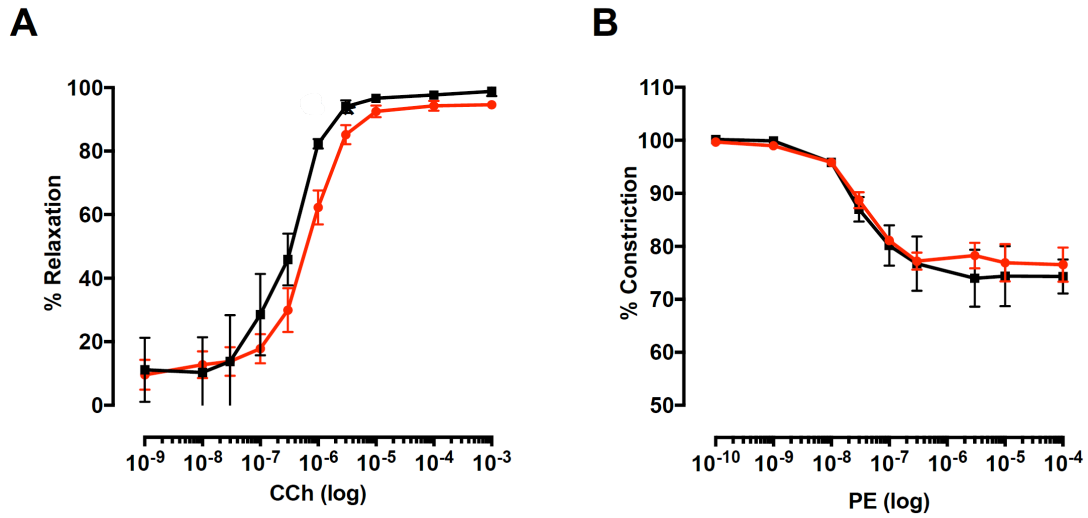
Supplemental Figure XIII. Vasoreactivity of large diameter arteries show no differences in reactivity. Carotid arteries (which exhibit few IEL holes) were cannulated and pressurized to 100 mmHg. **A**, CCh curves with EC Calr Δ/Δ (red, n=5 arteries from 4 mice) were compared to EC Calr fl/fl (black, n=3 arteries from 3 mice). **B**, PE curves with EC Calr Δ/Δ (red, n=3 arteries from 3 mice) were compared to EC Calr fl/fl (black, n=3 arteries from 3 mice). Comparisons were made between drugs doses using unparies student's t-tests.
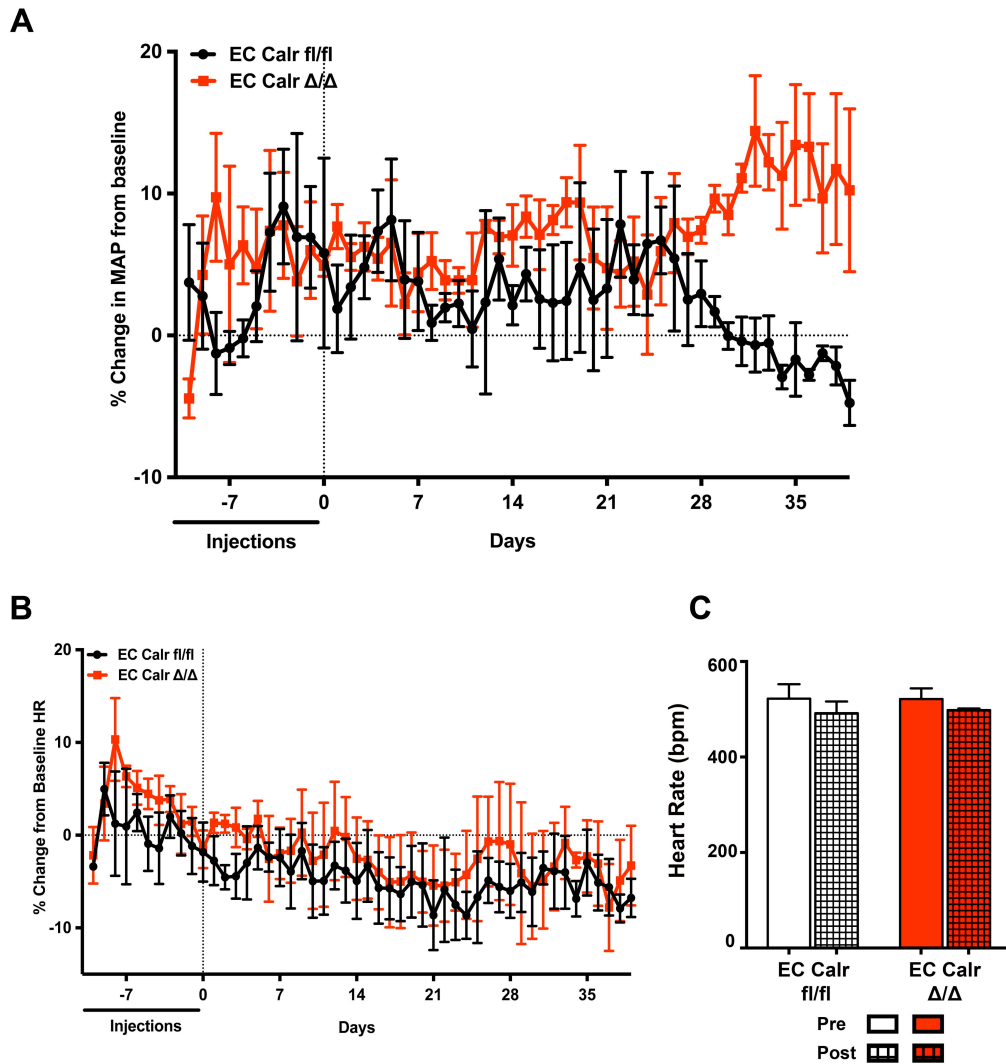
Supplemental Figure XIV. Time-course of average daily blood pressure and heart rate. The average daily change in **A**, mean arterial pressure (MAP) and **B**, heart rate compared to the pre-injection baseline measured via radiotelemetry catheters. Days -10 to -1 indicate injection with tamoxifen or vehicle control. Days 0-39 indicate post-EC Calr knockout (Days 0-39). **C**, Baseline absolute heart rate was not different. Comparisons were made between pre- and post- injection using paired student's t-tests.
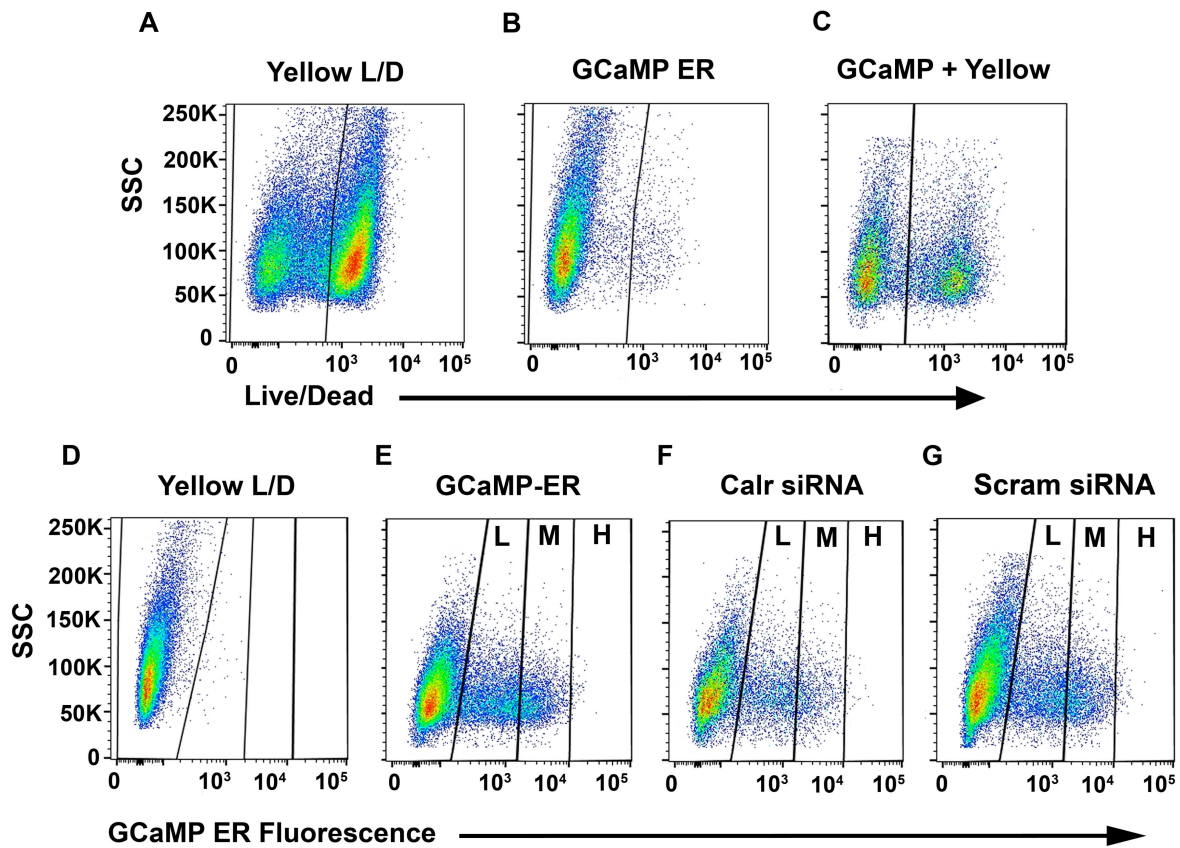
Supplemental Figure XV. GCaMP-ER flow cytometry gating strategy and representative results. Because GCaMP-ER fluorescence may change with apoptotic or dying cells, only live EC were analyzed. **A**, EC stained with yellow live/dead fluorescent dye (L/D). The dye is not taken up by cells with intact membranes, so increased fluorescence indicates non-viable cells. **B**, EC transfected with only GCaMP-ER do not have positive signal for live/dead dye. **C,** When EC transfected with GCaMP-ER are incubated with live/dead dye, a population of dead cells is seen in the right portion of the graph. **D,** Untransfected EC stained with yellow live/dead dye do not have signal for GCaMP-ER. **E,** EC transfected with GCaMP-ER and **F,** Calr siRNA or **G,** scrambled siRNA do not exhibit significant differences in low (L), medium (M) or high (H) GCaMP-ER fluorescence. Cell populations in the far left box do not exhibit GCaMP-ER signal. SSC= side scatter.
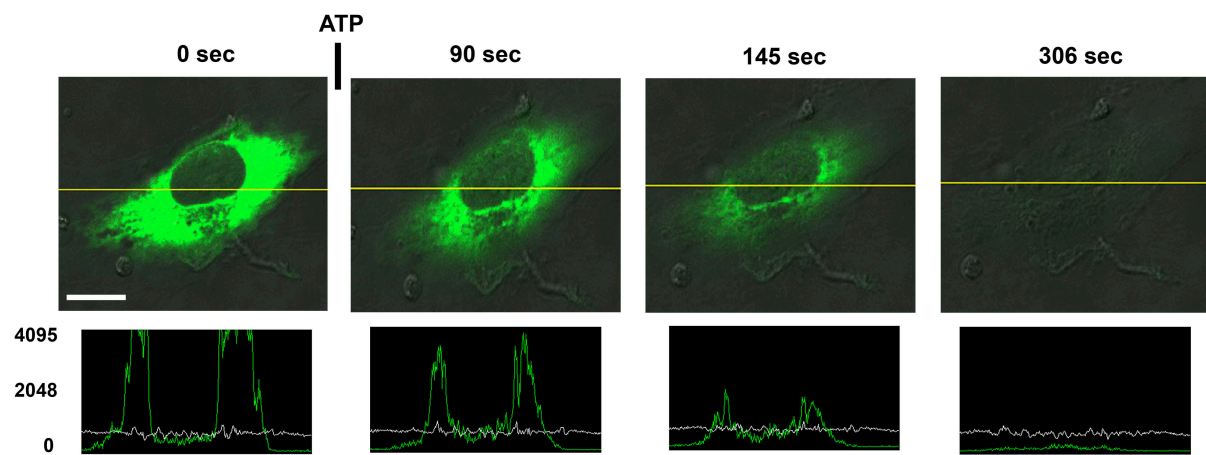
Supplemental Figure XVI. GCaMP-ER signal decreases after addition of 35uM ATP. Time-lapse images of an EC transfected with GCaMP-ER (green, visualized via GFP 488 laser) imaged on an upright confocal microscope over the course of 5 minutes. Line scans are indicated with yellow line and the fluorescent intensity is plotted below the image at each timepoint (Green is GCaMP-ER signal, grey is brightfield channel). Scale bar= 10μm.
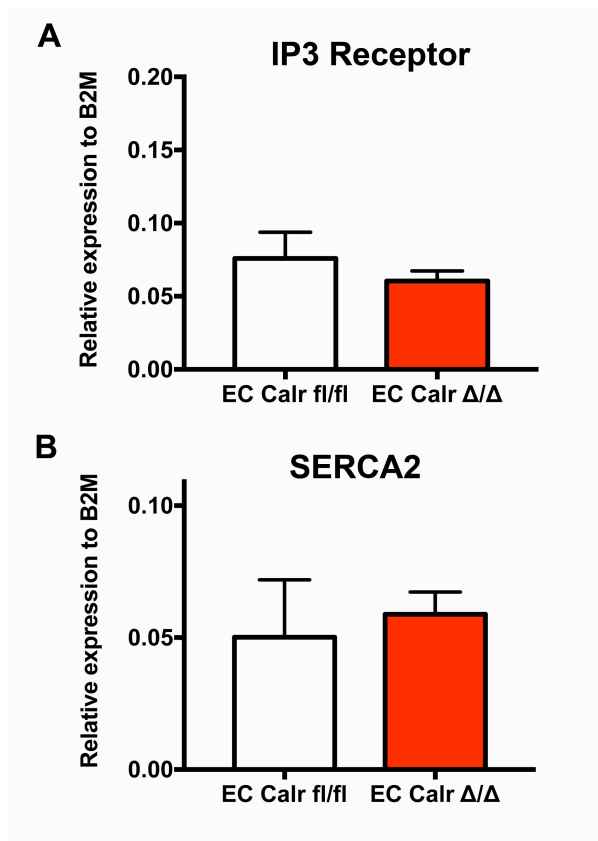
Supplemental Figure XVII. The relative expression of IP3R and SERCA2 does not change with EC Calr Δ/Δ. A, IP$_3$ Receptor expression is not different with endothelial calreticulin knockout (EC Calr fl/fl n=5, EC Calr Δ/Δ n=2). **B,** Serca2 expression is also not different (EC Calr fl/fl n=4, EC Calr Δ/Δ n=3). Comparisons were made using unpaired student's t-test.
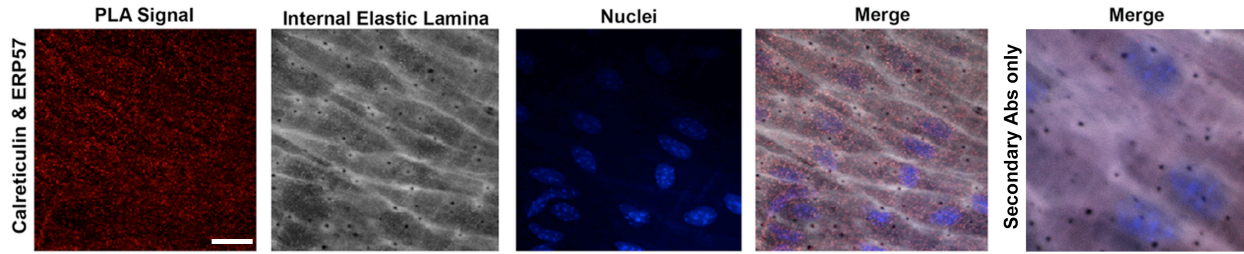
Supplemental Figure XVIII. Calreticulin and ERp57 preferentially associate in the EC monolayer of arteries. Proximity ligation assays (PLA; as previously described by us) demonstrate extensive co-localization in the EC monolayer of arteries (red punctate), but not in the holes in the IEL (HIEL). The IEL was counterstained with Alexa 647, and nuclei were revealed with DAPI. Secondary Ab controls used fluophore-conjugated IgG from both animals, but not primary Abs. Scale bar is 10 μm in PLA images with Calr and ERp57, and 5 μm in secondary Ab control.

A
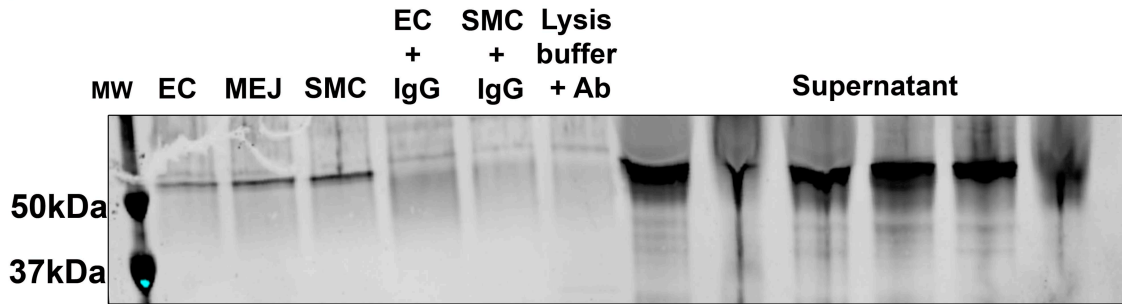
B

Protein	Accession Number	Molecular Weight (kDa)	EC	MEJ	SMC
78kDa Glucose regulated protein	P11021	72	7	1	1
Thrombospondin-1	P07996	129	1	2	0

Supplemental Figure XVIII. In vitro Calr co-immunoprecipitation shows differential interaction with proteins in EC monolayer versus MEJ. Primary human endothelial and smooth muscle cells were grown on opposite sides of a filter with 0.4m pores in which MEJ can form (vascular cell co-culture; "VCCC"). Three fractions from the VCCC were isolated (EC, MEJ and SMC), lysed, and immunoprecipitated with calreticulin antibody. The samples were then analyzed via mass spectrometry to obtain information about proteins that co-immunoprecipiated with calreticulin for label free, semi-quantitative comparisons. **A,** Representative immunoblot for calreticulin from calreticulin immunoprecipitation samples. EC/SMC + IgG: cell lysate incubated with only rabbit immunoglobulin G (no antibody), Lysis buffer + Ab: buffer incubated with only calreticulin antibody. The six supernatant lanes are ordered in the same left to right pattern as the six experimental samples. **B,** Table indicating two of the proteins identified via mass spectrometry from the immunoprecipitated calreticulin. Both proteins are known to interact with calreticulin. The relative spectral counts from the fractions give a semiquantitative count of the number of times the mass spectrometer was able to detect the molecule in the given amount of calreticulin protein. Thus, a larger spectral count indicates more identifications for the protein. The 78kDa Glucose regulated protein is also known as binding immunoglobulin protein (BiP).